



Electrochemical and X-ray photoelectron spectroscopic investigations of conductive polymers

Umesh Somaji Waware¹ · Ravi Arukula² · A. M. S. Hamouda¹ · Peter Kasak³

Received: 15 April 2019 / Revised: 26 August 2019 / Accepted: 3 September 2019 / Published online: 4 November 2019
© The Author(s) 2019

Abstract

We report the synthesis of high soluble poly(aniline-co-o-hydroxyaniline) copolymers with varying the amount of o-hydroxyaniline (20, 40, 60, and 80 %) and referred as PA-co-o-HA20, PA-co-o-HA40, PA-co-o-HA60, and PA-co-o-HA80 respectively. The chemical and structural composition of the polymers and copolymers were determined by XPS, UV–Vis, and FE-SEM analysis. Electrochemical studies of the as-prepared polymers showed two single-electron oxidations and two single-electron reductions reversibly at various scan rates ranging from 20 to 50 mV and results reveals that the current density of the copolymer was lesser than the conventional polyaniline (PA). This is due to increasing the hydroxyl (-OH) branching on the polymer backbone in the polymer chain. The current density decreases from PA-co-o-HA20 to PA-co-o-HA80 by increasing the weight percentage of o-hydroxyaniline in the polymeric backbone.

Keywords Polyaniline · Poly(aniline-co-o-hydroxyaniline) · XPS and cyclicvoltametry

Introduction

Electrode materials play an important role in energy conversion and storage devices [1]. Conducting polymers, carbon-based, and metal compounds are amongst the three important kinds used as electrode materials for energy conversion/storage devices. Conducting polymers (CPs), such as polypyrrole (PPy) and polyaniline (PA) and poly(3,4-ethylene dioxythiophene) (PEDOT), have immense attention in recent years because of their prospective uses in various fields such as supercapacitors, batteries, sensors, fuel cells, electrochromic devices, anticorrosive coatings, and electroactive polymers [2–10].

Amongst all conducting polymers, PA is a unique class material due to having low cost, easy preparation, commendable environmental stability, good electrical conductivity, and electrochemical activity [11, 12]. But, due to low processability and intractable nature of acid-doped PA that restricts the few applications in industry [13]; to overcome this problem, several researchers have been extensively improved the field in terms of synthesis, processability, and various applications [14–16]. The more significant strategies to attaining the good processability for conducting polyaniline are (i) to familiarize substituent groups on the phenyl ring [17, 18], (ii) self-doping (-SO₃H ring substituted) polyanilines [19, 20], and (iii) blending with conventional solvable polymers like poly(vinyl alcohol) [21]. As stated above, substituted polyanilines are soluble in common organic solvents [17]. Owing to distorted planar-conjugation, the substituent conducting polyaniline attains the less conductivity. To improve the processability and conductivity in conducting polymers, the copolymers of aniline and substituted anilines have been introduced. Numerous aniline copolymers are well known from the literature [22, 23]. However, to the best of our knowledge, only a few studies report the extensive structural elucidation of conducting polyaniline copolymer.

The foremost studies on the structural interpretation of polyaniline or copolyanilines are mainly, optical absorption [24, 25], electron spin resonance [26], nuclear magnetic

Electronic supplementary material The online version of this article (<https://doi.org/10.1007/s11581-019-03250-8>) contains supplementary material, which is available to authorized users.

✉ Umesh Somaji Waware
uswaware@gmail.com

¹ Department of Mechanical and Industrial Engineering, Qatar University, P.O. Box 2713, Doha, Qatar

² Department of Chemistry, GITAM University, Hyderabad, India

³ Center for Advanced Materials, Qatar University, P.O. Box 2713, Doha, Qatar

resonance [27], electrochemical activity [28] measurements, and Raman and IR studies [29–31] of polymers prepared under various conditions. The huge experimental and theoretical work have done on different forms of polyaniline has; however, not absolutely determined the molecular structure of the polymer and copolymers. However, MacDiarmid et al. [32] and Baughman et al. [33] were proposed a highly delocalized configuration structures of polyaniline, wherein the polyemeraldine salt (ES) is considered to be made up of equivalent nitrogen atoms, and the six-membered ring structure and the C-N bonds are considered equivalent in all respects. Still, there is a challenge to extensive structural elucidation of conducting polyaniline copolymer using electronic studies like X-ray photoelectronic spectroscopy (XPS).

The intention of the present work is to investigate detailed cyclic voltammetry and XPS of PA, P-*o*-HA, and high soluble poly(aniline-co-*o*-hydroxyaniline) copolymers. The XPS is a dominant surface analysis tool extensively used in polymers; polymer blending and composites field [34] and this method reveals the composition, oxidation state, and chemical bonding of atoms found in a near-surface region of the thickness of 5 to 10 nm. The chemical composition can be found based on the binding energies and peak intensity. The formal characterizations of PA, P-*o*-HA, and high soluble poly(aniline-co-*o*-hydroxyaniline) copolymers, electrochemical, and XPS study were thoroughly investigated as follows.

Experimental section

Chemicals and materials

Aniline, *o*-hydroxyaniline, and ammonium persulfate were purchased from the Sigma-Aldrich and used as received. Analytical grade hydrochloric (HCl) acid and spectroscopic grade dimethylformamide (DMF), (THF), *N*-methylpyrrolidone (NMP), and methanol were used as received. Double-distilled (DW) water was used in the preparation of aqueous solutions.

Synthesis

Synthesis of PA and P-*o*-HA

Polyaniline (PA) and poly(*o*-hydroxyaniline) P-*o*-HA were synthesized by oxidation of aniline and *o*-hydroxyaniline separately with ammonium persulfate in 1 M hydrochloric acid according to modified procedure reported [22]. In a typical reaction, aniline (20 mmol, 1.86 g) was added to 200 mL of 1 M HCl and the mixture was cooled to 0–4 °C in an ice bath. An ice-cold solution of 20 mmol (4.56 g) ammonium persulfate dissolved in 200 ml of 1 M HCl was then added dropwise into the monomer solution with constant stirring under

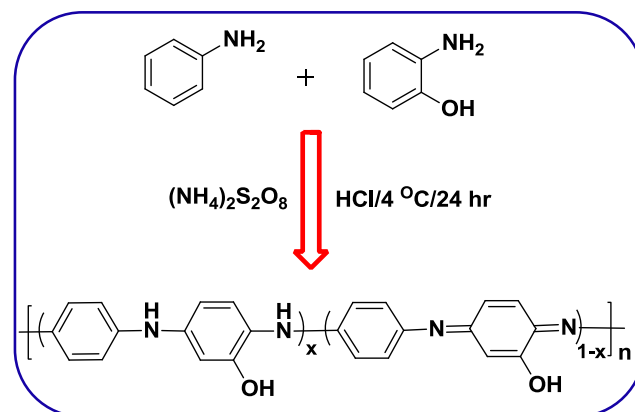
nitrogen atmosphere at 0–4 °C. The reaction mixture was further stirred for another 5 h and aged at room temperature for 24 h which resulted in a greenish precipitate of the polymer in emeraldine salt form (PA hydrochloride). It was filtered and washed with small volumes of 1 M HCl and dried in an air oven for 8 h at 80 °C. The base form of the polymer was obtained by treatment of emeraldine salt with 1 M NH₄OH solution and kept for 24 h at room temperature. The separated base was washed with distilled water, filtered, and air-dried. Similarly, poly(*o*-hydroxyaniline), P-*o*-HA was obtained by oxidative polymerization of *o*-hydroxyaniline using ammonium persulfate. The final product of the polymer powder obtained was brown in color.

Synthesis of copolymers (PA-co-*o*-HA)

Copolymers of aniline and *o*-hydroxyaniline (PA-co-*o*-HA) were obtained by chemical oxidative coupling of the monomers in 1 M HCl using ammonium persulfate in a similar way. Different copolymers were prepared by varying the amount of *o*-hydroxyaniline, namely 20, 40, 60, and 80 %. The copolymers with 20, 40, 60, 80 % *o*-hydroxyaniline will be referred from here on as PA-co-*o*-HA20, PA-co-*o*-HA 40, PA-co-*o*-HA 60, and PA-co-*o*-HA 80 respectively. The structure and synthetic procedure of copolymers (PA-co-*o*-HA X) are shown in Scheme 1 and the 3D Chemical structures of PA, P-*o*-HA, and copolymers were shown in Scheme 2.

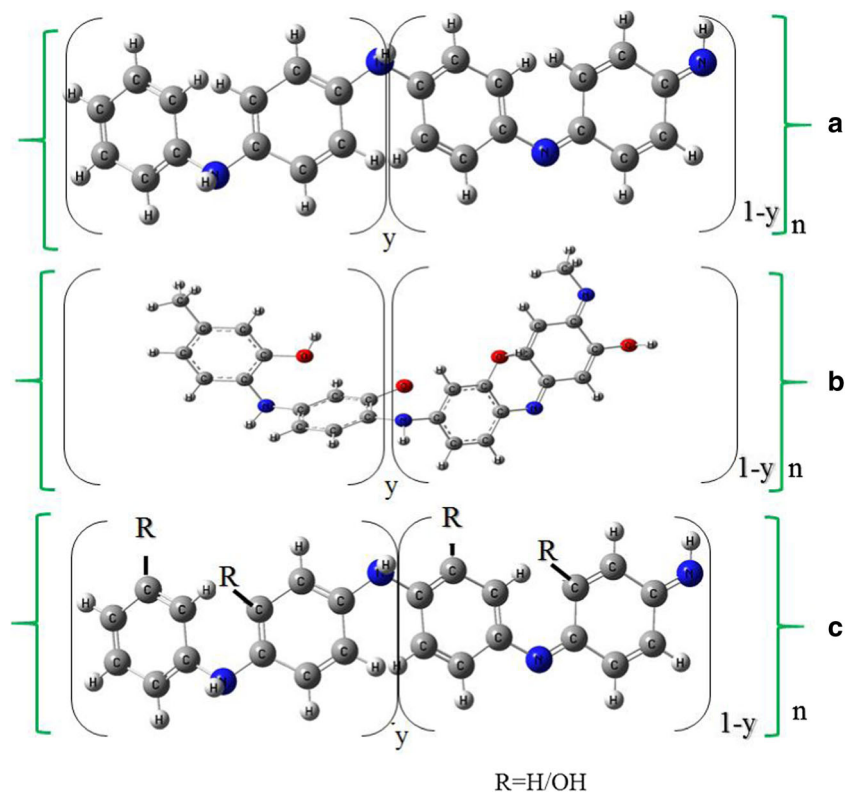
Modification of glassy carbon electrode

First, the working electrode, glassy carbon electrode (GCE) was polished with 1.0 μm alumina slurry and sonicated in DW. The cleaned GCE was subsequently dried using a purified nitrogen stream. The casting solution was prepared in DMF solvent with a concentration of 5 mg/mL. In order to obtain a homogeneous dispersion of the solution was



Scheme 1 Synthetic route for the preparation of HCl-doped polyaniline, poly(*o*-hydroxyaniline), and its various copolymers

Scheme 2 3D chemical structures of **a** polyaniline PA, **b** poly(*o*-hydroxyaniline) P-*o*-HA, **c** poly(aniline-co-*o*-hydroxyaniline) derivatives PA-co-*o*-HA



sonicated for 5 min. The modified electrode was prepared by a simple drop-casting method, by pipetting a volume of 10 μL on the GCE and dried at room temperature under vacuum condition.

Characterization

Cyclic voltammetry

All electrochemical tests were performed on a laboratory potentiostat (Gamry 3000, USA) with a glassy carbon electrode (GCE, $d = 3$ mm, Bioanalytical systems, USA) used as a working electrode. Ag/AgCl/3 M KCl electrode and Pt electrode (Bioanalytical systems, USA) were applied in a three-electrode cell system as reference and counter electrodes respectively. Cyclic voltammetric measurements were acquired under Gamry Instruments Framework software, and data acquired were evaluated using Echem Analyst and OriginPro 8.

Cyclic voltammetry test was conducted in 0.1 M H_2SO_4 acid solution as the electrolyte under N_2 atmosphere, in the potential range from -0.4 to 0.8 V at a scan rate of 100 mVs^{-1} . Scan rate influence was also studied under similar conditions except for, scan rates varied at 10, 20, 30, 40, and 50 mVs^{-1} in the potential range between -0.2 and 0.7 V.

XPS studies

The XPS signals on the powdered sample were recorded using AXIS ULTRA DLD (Kratos Analytical Ltd., UK) equipped with an Al K α X-ray source. The spectra were acquired in the constant analyzer energy mode with pass energy of 160 eV, 10 kV, and 10 mA emission current for the survey. The individual scans were performed with pass energy of 10 eV, 15 kV, and 15 mA emissions current. The Vision Manager 2 software was used for digital acquisition and data processing. Spectral calibration was determined using the automated calibration routine and the internal C1s standard. Scanning electron micrographs are taken with JEOL-6700 field emission microscope to study the morphology of the polymers.

In 100 ml of DMF solvent, the solubility of PA and PA-co-*o*-HA derivatives in the powder form is to be determined by dissolving 10 mg of the polymer and allowed to disperse homogeneously. The dispersion is aged for few hours at the room temperature of 25 $^\circ\text{C}$; the polymer dispersion is now being filtered through sintered glass crucible (porosity 2 μm).

UV-Visible

UV-Visible absorption spectra of the polymer samples in NMP solvent were recorded at room temperature on a

Thermo Spectronic Genesys2 Research Grade Spectrophotometer.

Results and discussion

Solubility test

Processability plays an important role in conducting polymers and their applications. The solubility of PA, P-o-HA, and the copolymers dissolved individually in THF solvent and were presented in Table 1. The data reveals that the solubility of conventional PA (8.78×10^{-2} (W/V %), (g/dL)) is lesser than the P-o-HA, and the copolymers. The homopolymer (P-o-HA) solubility is better than ten times (90.78×10^{-2} (W/V %), (g/dL)) to PA. However, the copolymer solubility increases gradually with increasing the weight percentage of ortho hydroxy aniline units in the polymer backbone and attained the maximum solubility (73.35×10^{-2} to 87.56×10^{-2} (W/V %), (g/dL)). In conclusion, the solubility of the PA is lesser than that of P-o-HA and copolymers, and the solubility ranges of the copolymers were in between the PA and homopolymer (P-o-HA). P-o-HA and copolymers were attaining remarkable solubility due to the presence of –OH (hydrogen bonding) group onto the polymer backbone, and which provide the more polar nature to the copolymer.

Morphological properties

The FE-SEM images of synthesized PA and PA-co-o-HA copolymer of magnification 80 k are depicted in Fig. 1. The average particle size of the PA and copolymer is around 0.5 to 1 μm . The microscopy revealed rough topology with clusters surfacing on the top for the as-prepared PA (Fig. 1a). Interesting morphological changes occur in case of PA-co-o-HA copolymer. Regular and perfectly shaped cabbage flower globules are developed (Fig. 1b). These globules formation could have taken place because of the hydrophobic nature of polyaniline particles and severe stirring conditions which catered the doped polymer's transformation into a globular structure.

Table 1 Solubility data of both homopolymers and copolymers

| Polymers derivatives HCl salt | Solubility (W/V %), (g/dL), THF |
|-------------------------------|---------------------------------|
| P-o-HA | 90.78×10^{-2} |
| PA-co-o-HA20 | 73.35×10^{-2} |
| PA-co-o-HA40 | 81.00×10^{-2} |
| PA-co-o-HA60 | 85.96×10^{-2} |
| PA-co-o-HA80 | 87.56×10^{-2} |
| PA | 8.78×10^{-2} |

Structural properties

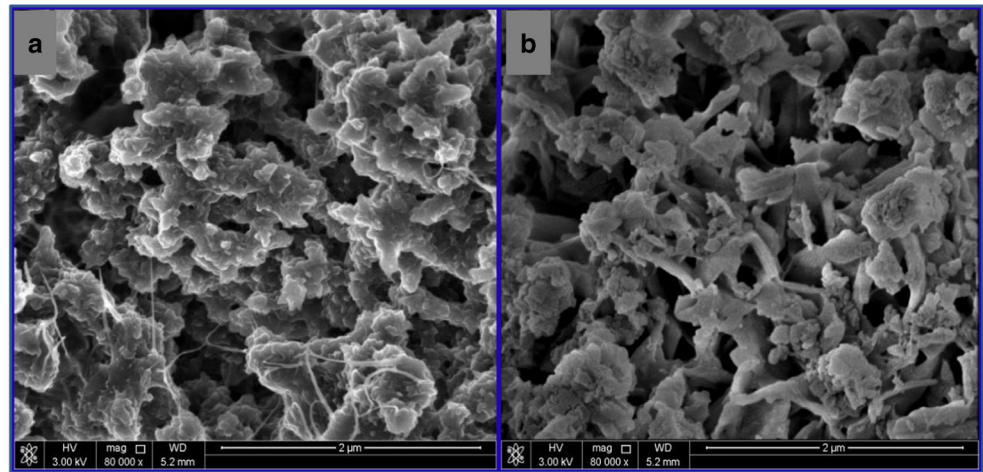
UV–Vis absorption study

The UV–Vis electronic absorption spectroscopy is an important tool for conducting polymers and their composites to recognizing the conducting and insulating states. The PA, P-o-HA, and copolymers dissolved in NMP and spectra recorded at room temperature in the range of 250–900 nm. The spectra were shown in Fig. S1 [supplementary material]. The PA, P-o-HA, and copolymers showed two visible absorption bands around 310 and 580 nm in NMP solvent [35]. The lower wavelength band is attributed to the π – π^* transition of the conjugated ring systems and the higher wavelength band is assigned to the n – π^* exciton transition between the highest occupied molecular orbital (HOMO) of the benzenoid ring and the lowest unoccupied molecular orbital (LUMO) in the quinoid ring (i.e., benzenoid to quinoid excitonic transition). The obtained data for PANI, P-o-HA, and copolymers were much closed with other researchers [36, 37]. Decreasing the intensity of lower band wavelength may be due to growing hydroxy branching in the polymer backbone, which lacks the π – π^* conjugation in between phenyl rings.

XPS study

XPS was examined to identify chemical element presence and chemical character at particular elements. The survey spectra of PA, P-o-HA, and copolymer polymers reveal that presence of expected elements in all samples and it is in good agreement with feeding in samples (Fig. 2). Figure 3 shows the N1s spectra of all three samples and Fig. 3a represents the N 1s spectra for polyaniline and the curve deconvoluted into three peaks with 399.1, 400.8, and 402.1 eV corresponding to C–N, neutral/tertiary amine (C=N) and quaternary amine/protonated imine (C=NH⁺) respectively. Similarly, in Fig. 3b, c), the same pattern was observed for P-o-HA and copolymer at 398.2, 399.5, and 401.5 eV and 398.8, 399.7, and 402.3 eV respectively. The obtained data for N 1s for all the three above samples were close to literature. The binding energies for C1s spectra of PA, P-o-HA, and copolymer observed at \sim 284.2, 285.8, 286.3, and 287.6 eV ascribed to C–C, C=N, C=NH⁺, and C=O functionality, respectively (Fig. 4a–c). The first integral detected at \sim 284.2 eV is attributed to the neutral C–C bonds in the polymer backbone. The second component at \sim 285.8 eV can be consigned to the carbon bonded with neutral nitrogen atoms (C=N). Third peak can be ascribed to the carbon atoms bonded to charged nitrogen atoms (C=NH⁺). The highest binding energy \sim 287 eV is characteristic peak for the carbon connected with oxygen (C=O), and the C=O functional groups are assigned to be present in PANI, P-o-HA, and copolymer due to the formation of benzoquinone (BQ) and hydroquinone (HQ) as degradation

Fig. 1 SEM images of **a** PA and **b** PA-co-o-HA copolymer



products [38]. The O1s spectra were not considered for further analysis of synthesized polymers since it is extremely influenced by moisture and oxide residue impurities that are common for XPS analysis. Finally, this XPS data also suggests that the formation PA, P-o-HA, and copolymer in emeraldine salt (ES) form [39].

Electrochemical performance

The electrical conductivity and electrochemical properties are most significant properties for the conducting polyaniline. The as-prepared PA, P-o-HA, and copolymers were investigated for their electrochemical activity by CV using GCE as a

working electrode in a three-electrode system. The electrochemical tests were performed in 0.1 M H₂SO₄ acid solution as the electrolyte under N₂ inert atmosphere, in the potential window from −0.4 to 0.8 V at different scan rates ranging from 20 to 50 mV mVs^{−1}. As shown in Fig. 5, the conventional polyaniline (PA) shows two forward peaks at 0.286 (peak 1) and 0.540 V (peak 2) and two backward (reverse) peaks at 0.286 and 0.540 V corresponding to two single-electron oxidations and two-single electron reductions reversibly at different scan rates. The similar pattern was observed in P-o-HA homopolymer as shown in Fig. 5a. Similarly, the first and second oxidation peaks for copolymer are observed at 0.246 V and 0.445 V, very close to PA and P-o-HA. The peak

Fig. 2 XPS survey for **a** PA, **b** P-o-HA, **c** copolymer

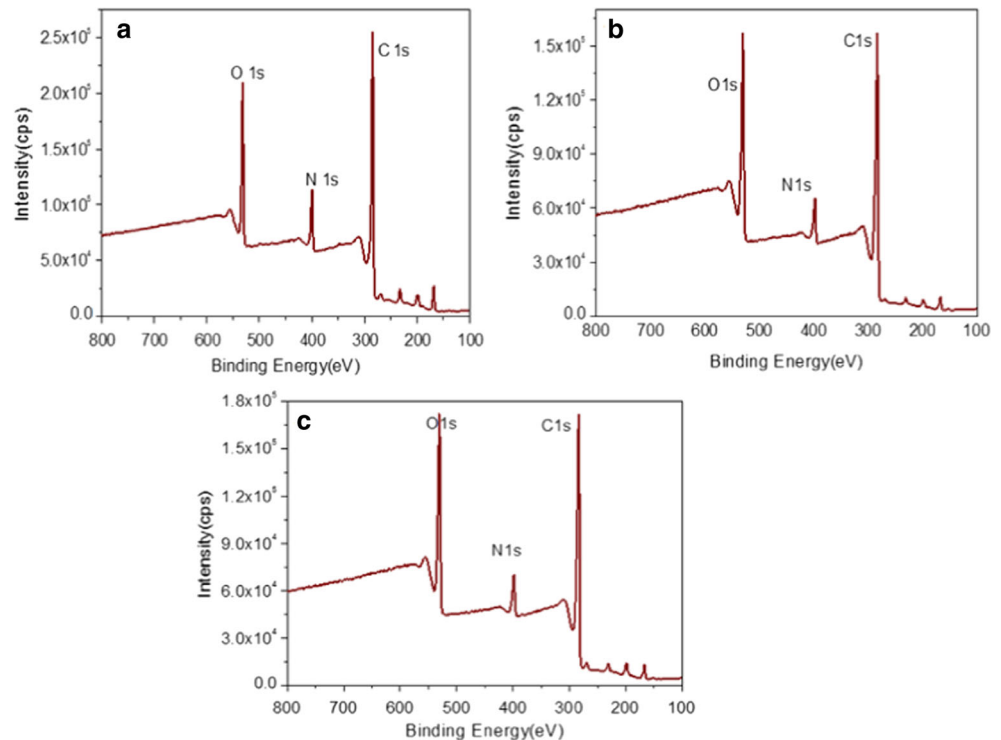
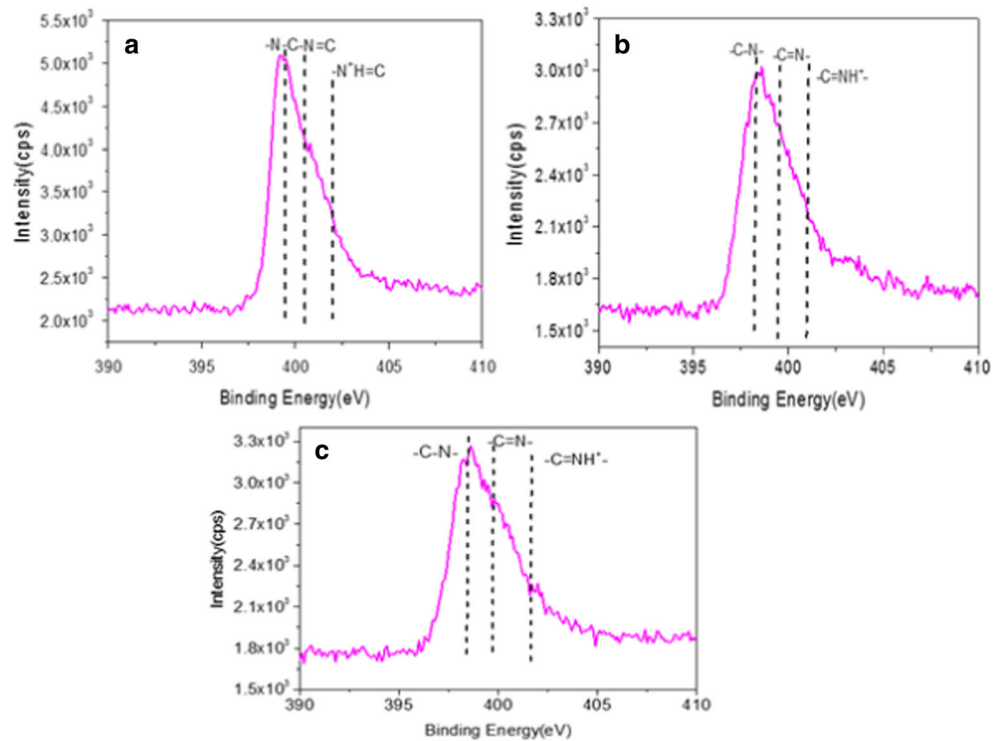


Fig. 3 XPS spectra for N 1s region for **a** PA, **b** P-o-HA, **c** copolymer



current of PA is higher compared to P-o-HA and which in turn is higher when compared to the copolymer. This is due to increasing the hydroxyl (-OH) branching on the polymer backbone in the polymer chain. In general, while branching increases in copolymers the planarity of the phenyl ring will

be reduced, this leads to the decreasing in conjugation and conductivity as well. The current density decreases from PA-co-o-HA20 to PA-co-o-HA80 by increasing the weight percentage of o-hydroxyaniline in the polymeric backbone. The oxidation peaks correspond to the transitions from

Fig. 4 XPS spectra for C 1s region for **a** PA, **b** P-o-HA, **c** copolymer

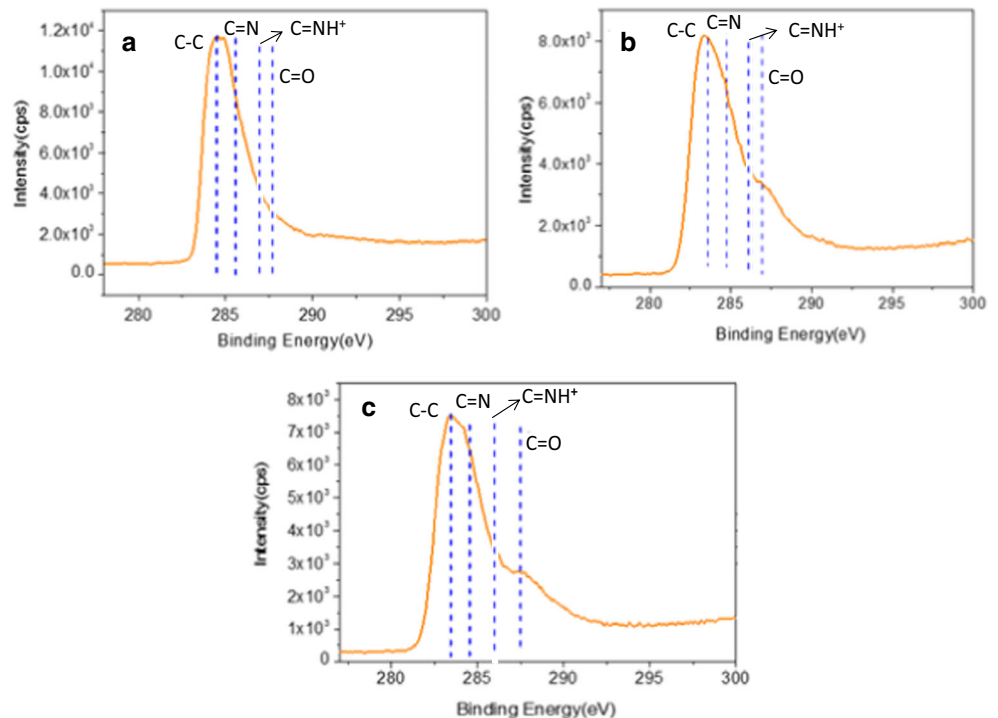
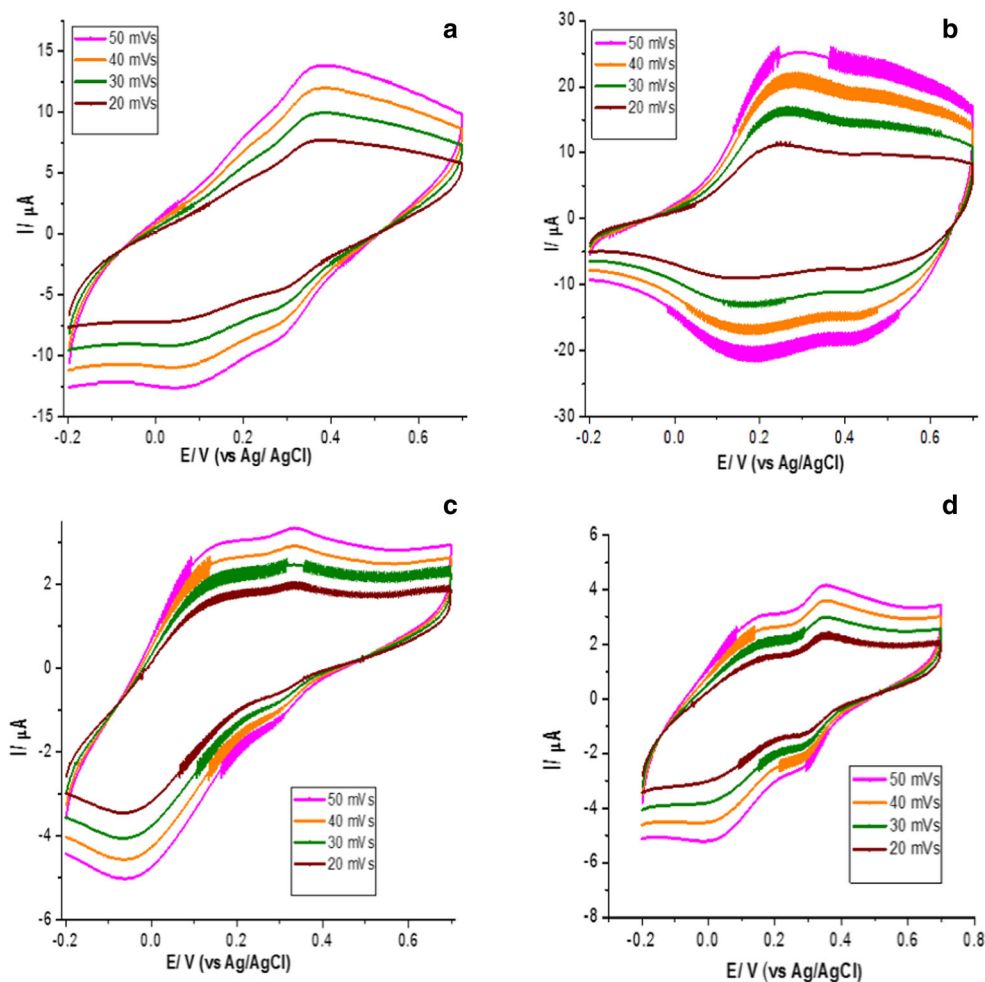


Fig. 5 Cyclic voltammetry scan of **a** P-o-HA, **b** PA, **c** PA-co-o-HA 80, **d** PA-co-o-HA 20



leucoemeraldine base (LEB) to emeraldine base (EB) oxidation state and EB to pernigraniline (PA) oxidation state, respectively.

Conclusions

In summary, using a chemical oxidative polymerization, we have successfully synthesized poly(aniline-co-o-hydroxyaniline) copolymers with varying the amount of o-hydroxyaniline (20, 40, 60, and 80 %) and named as PA-co-o-HA20, PA-co-o-HA40, PA-co-o-HA60, and PA-co-o-HA80 respectively. The possible formation of polymers and copolymer structures were explained in detail with the help of FE-SEM, UV, and XPS analysis. The solubility of PA, P-o-HA, and the copolymers dissolved individually in THF solvent and the solubility of conventional PA (8.78×10^{-2} (W/V %), (g/dL)) is lesser than the P-o-HA, and the copolymers. The homopolymer (P-o-HA) solubility is better than ten times to PA. However, the copolymer solubility increases gradually

with increasing the weight percentage of ortho hydroxy aniline units in the polymer backbone and attained the maximum solubility (74.88×10^{-2} to 87.56×10^{-2} (W/V %), (g/dL)). From cyclic voltammograms, the peak current of PA is higher compared to P-o-HA and which in turn is higher when compared to copolymer and the current density decreases from PA-co-o-HA20 to PA-co-o-HA80 by increasing the weight percentage of o-hydroxyaniline in polymeric backbone.

Acknowledgements We gratefully acknowledge the Qatar University, Doha, for providing necessary research funding. We also acknowledge the instrumentation facilities provided at CLU and CAM of Qatar University, Doha.

Open Access This article is distributed under the terms of the Creative Commons Attribution 4.0 International License (<http://creativecommons.org/licenses/by/4.0/>), which permits unrestricted use, distribution, and reproduction in any medium, provided you give appropriate credit to the original author(s) and the source, provide a link to the Creative Commons license, and indicate if changes were made.

References

1. Wang H, Jianyi L, Xiang Shen Z (2016) *J Sci Adv Mater Devices* 1: 225–255
2. Sangodkar H, Sukeerthi S, Srinivasa RS, Lal R, Contractor AQ (1996) *Anal Chem* 68
3. Langer JJ, Langer RK (2005) *Rev. Adv Mater Sci* 10:434
4. Bhadra S, Khastgir D, Singha NK, Lee JH (2009) *Prog Polym Sci* 34:783e810
5. Lu WK, Elsenbaumer RL, Wessling B (1995) *Synth Met* 71:2163
6. Ahmad N, MacDiarmid AG (1996) *Synth Met* 78:103
7. Ravi A, Mohanraj V, Kim AR, Yoo DJ (2019) *J Alloys Compd* 771: 477–488
8. Wang YZ, Gebler DD, Lin LB, Blatchford JW, Jessen SW, Wang HL, Epstein AJ (1996) *Appl Phys Lett* 68:894
9. Chen SA, Chuang KR, Chao CI, Lee HT (1996) *Synth Met* 82:207
10. MacDiarmid AG, Yang LS, Huang WS, Humphrey BD (1987) *Synth Met* 18:393
11. Kang ET, Neoh KG, Tan KL (1992) *Surf Interface Anal* 19:33
12. MacDiarmid AG, Chiang JC, Richter AF, Epstein AJ (1987) *Synth Met* 18:285
13. Kinlen PJ, Frushour BG, Ding Y, Menon V (1999) *Synth Met* 101: 758–761
14. Skotheim TA (1986) *Handbook of conducting polymers*, vol 1. Marcel Dekker, New York, p and 2
15. Trivedi DC, Nalwa HS (1997) *Handbook of organic conductive molecules and polymers*, vol 2. Wiley, Chichester
16. Park SM, Nalwa HS (1997) *Handbook of organic conductive molecules and polymers*, vol 3. Wiley, Chichester
17. Macinnes D, Funt BL (1988) *Synth Met* 25:235–242
18. Gazotti WA Jr, de Paoli MA (1996) *Synth Met* 80:263–269
19. Yue J, Wang ZH, Cromack KR, Epstein AJ, MacDiarmid AG (1991) *J Am Chem Soc* 113:2665–2671
20. Wei XL, Wang YZ, Long SM, Bobeczko C, Epstein AJ (1996) *J Am Chem Soc* 118:2545–2555
21. Dalas E (1992) *J Mater Sci* 27:453–457
22. Waware US, Summers GJ, Mohd R, Hamouda AMS (2017) *Ionics*. 24:118
23. Clioi HJ, Kim JW, To K (1999) *Synth Met* 101:697–698
24. McManus PM, Cushman RJ, Yang SC (1987) *J Phys Chem* 91:744
25. Stafstrm S, Das JL, Epstein AJ, Woo HS, Tanner DB, Huang WS, MacDiarmid AG (1987) *Phys Rev Lett* 59:1464
26. Kaya M, Kitani A, Sasaki K (1986) *Chem Lett*:147
27. Stafstrm S, SjSgren B, Wennerstr SO, Hjertberg T (1986) *Synth Met* 16:31
28. Genies EM, Lapkowski MJ (1987) *Electroanal Chem* 220:67
29. Furukawa Y, Hara T, Hyodo Y, Harada I (1986) *Synth Met* 16:189
30. Ohira M, Sakai T, Takeuchi M, Kobayashi Y, Tsuji M (1987) *Synth Met* 18:347
31. Regina M, Gediminas N, Albertas M (2019) *Synth. Met*, vol 248, pp 35–44
32. Chiang JC, MacDiarmid AG (1986) *Synth Met* 13:193
33. Baughman RH, Wolf JF, Eckhardt H, Shacklette LW (1988) *Synth Met* 25:121
34. Azmi R, Trouillet V, Strafela M, Ulrich S, Ehrenberg H, Bruns M (2017) *Surf Interface Anal*:1–9
35. Yang Z, Wang X, Yang Y, Liao Y, Wei Y, Xie X (2010) *Langmuir* 26:9386–9392
36. Jing X, Wang Y, Wu D, Qiang J (2007) *Ultrason Sonochem* 14:75–80
37. Manohar SK, MacDiarmid AG (1991) *Synth Met* 41:711–714
38. Sebastian G, Anna K, Mats F, Krzysztof L, Jerzy JL (2008) *Solid State Ionics* 179:2234–2239
39. Rohit RG, Amir HFN, Marlies H, Debra JS, Nanjundan AK, Zhao XS (2017) *J Mater Chem A* 5:22186–22192

Publisher's note Springer Nature remains neutral with regard to jurisdictional claims in published maps and institutional affiliations.